

# NUMERICAL STUDIES ON ELECTRON BEAM QUALITY OPTIMIZATION IN A LASER-DRIVEN PLASMA ACCELERATOR WITH EXTERNAL INJECTION AT SINBAD FOR ATHENA<sub>e</sub>

E. N. Svystun<sup>†</sup>, R. W. Assmann, U. Dorda, B. Marchetti, A. Martinez de la Ossa,  
Deutsches Elektronen-Synchrotron, DESY, 22607 Hamburg, Germany

## Abstract

Nowadays the electron beams produced in plasma-based accelerators (PBAs) are of sufficient energy for multi-GeV applications. However, to allow PBAs to be usable for demanding applications such as Free-Electron Lasers, the quality and stability of plasma-accelerated beams have to be improved. We present numerical studies on acceleration of an RF-generated electron beam with a charge of 0.8 pC and initial mean energy of 100 MeV to GeV energies by a laser-plasma accelerator. This acceleration scheme is planned to be tested experimentally within the framework of the ATHENA<sub>e</sub> (Accelerator Technology HELmholtz iNfrAstructure) project at the SINBAD (Short INnovative Bunches and Accelerators at DESY) facility at DESY, Hamburg. Electron beam injection, acceleration and extraction from the plasma are investigated through start-to-end 3D simulations. The effect of the injection phase on the accelerated beam quality is investigated through tolerance studies on the arrival-time jitter between the electron beam and the external laser.

## INTRODUCTION

Laser-plasma accelerators (LPAs) are considered one of the most promising candidates for future compact accelerators and light sources due to their enhanced accelerating gradients of ~100 MV/m [1] and the significant progress in laser technology made in the past decade [2, 3]. One of the key milestones in the realization of laser wakefield acceleration (LWFA) as an attractive and realistic technology for most modern applications will be the demonstration of delivering plasma-accelerated electron beams with sufficient quality and stability. External injection of an RF-generated electron beam is one of the important and promising technologies for the production of high-quality beams in LPAs. In this acceleration scheme, well-developed technologies of conventional electron linacs allow the precise phase-space manipulation of the electron beam before injection into a laser-driven plasma wakefield. This in turn enables the possibility of electron beam dynamics to be optimized inside a plasma acceleration stage. Considerable experimental [4-7] and theoretical [8-11] progress has been made in the field of LWFA with external injection in the past decades.

In this paper we present an extension of studies reported in [12] on the optimization of the potential experimental setup and the electron beam quality from external injection in laser-driven plasma acceleration at SINBAD [13], considering the full 6D phase space distribution of the electron

beam. Moreover, we have also investigated the effect of the injection phase on the accelerated beam quality through tolerance studies on the arrival-time jitter between the electron beam and the external laser. These studies have been carried out within the framework of the ATHENA<sub>e</sub> flagship project. ATHENA is a new research and development platform, which will provide the infrastructure required for bringing compact and cost-effective plasma accelerators to user readiness with applications in science and medicine. ATHENA is structured into two technology flagship projects and several application projects. The ATHENA<sub>e</sub> flagship project dedicated to electron acceleration will be hosted at the SINBAD facility at the DESY Hamburg campus. ATHENA<sub>e</sub> aims at transforming the existing plasma acceleration proof-of-principle results into novel, cost-efficient accelerator technology with a sufficient beam quality for various applications in the Helmholtz Association of German Research Centers and beyond.

## RESULTS AND DISCUSSION

### *Potential Experimental Setup for LWFA with External Injection at SINBAD for ATHENA<sub>e</sub>*

One of the main goals of the planned plasma experiments at SINBAD will be the controlled injection of an RF-generated electron beam into a plasma stage and its quality-preserving acceleration to GeV energy. The external witness beam will be injected in the accelerating wakefield excited in a plasma by a laser pulse generated by a Ti:Sapphire-based laser system. The electron beam will be produced by the SINBAD-ARES linac [14]. The ARES linac (Accelerator Research Experiment at Sinbad) is a normal-conducting 100 MeV S-band linear accelerator. ARES is foreseen to provide ultrashort (fs and sub-fs duration) electron beams with low charge (0.5-30 pC) and arrival-time stability less than 10 fs RMS [15].

### *Simulation Parameters*

Various basic working points (WPs) were simulated with ASTRA and IMPACT-T to cover the design ranges of beam parameters for the ARES linac [16]. In this paper we consider WP1 designed to reach sub-fs bunch length with the smallest possible beam arrival-time jitter. A full set of initial electron beam parameters is given in Table 1.

In all completed simulations the laser pulse defocusing was mitigated by external guiding of the laser pulse implemented by tailoring the transverse plasma density profile. This allowed the effective acceleration region to be extended and the injected witness beam to be accelerated to GeV energies.

<sup>†</sup> email address: elena.svystun@desy.de

Table 1: Electron Beam Parameters at the Plasma Entrance

Charge, $Q$ [pC]	0.8
Peak current, $I_{peak}$ [kA]	0.55
Mean energy, $\bar{E}$ [MeV]	100
Relative energy spread, $\Delta E/\bar{E}$ [%]	0.2
Longitudinal RMS size, $\sigma_{z,rms}$ [ $\mu\text{m}$ ]	0.155 (0.5 fs)
Horizontal RMS size, $\sigma_{x,rms}$ [ $\mu\text{m}$ ]	0.80
Vertical RMS size, $\sigma_{y,rms}$ [ $\mu\text{m}$ ]	0.73
Normalized horizontal emittance, $\varepsilon_{n,x}$ [ $\mu\text{m}$ ]	0.11
Normalized vertical emittance, $\varepsilon_{n,y}$ [ $\mu\text{m}$ ]	0.10
Beta-function, $\beta_x$ [mm]	1.13
Beta-function, $\beta_y$ [mm]	1.00
Beam density, $n_b$ [ $\text{cm}^{-3}$ ]	$34.6 \times 10^{17}$

The laser pulse parameters were defined as follows: pulse length  $\tau_l = 25$  fs (FWHM); spot size  $w_0 = 42.47$   $\mu\text{m}$ ; peak normalized vector potential  $a_0 = 1.8$ ; wavelength  $\lambda_l = 800$  nm. The laser transverse and temporal profiles are Gaussian. The laser pulse and the electron beam are injected collinearly into a plasma channel with a radially parabolic density profile of the form  $n(r) = n_0 + \Delta n(r/r_{ch})^2$ , where the channel depth  $\Delta n = 0.626n_0$ , the channel width  $r_{ch} = 42.47$   $\mu\text{m}$  and the on-axis plasma density  $n_0 = 1 \times 10^{17}$   $\text{cm}^{-3}$ . The plasma wavelength is  $\lambda_p = 106$   $\mu\text{m}$  and the plasma skin depth is  $c/\omega_p = k_p^{-1} = 16.8$   $\mu\text{m}$ , with the plasma frequency given by  $\omega_p = (n_0 e^2 / \varepsilon_0 m_e)^{1/2}$ , where  $c$  is the speed of light,  $k_p$  is the plasma wave number,  $e$  is the electron charge,  $\varepsilon_0$  is the vacuum permittivity and  $m_e$  is the electron mass. The temporal offset between the electron beam center and the peak of the laser pulse envelope  $\Delta \tau_{eb/lp}$  is equal to 211.6 fs (63.4  $\mu\text{m}$ ), 193.8 fs (58.1  $\mu\text{m}$ ) or 176 fs (52.8  $\mu\text{m}$ ) depending on the case. For the considered parameter set, a temporal electron beam-laser offset of 211.6 fs corresponds to the case when the external beam is located in the position of maximum accelerating field amplitude (near the on-crest acceleration phase).

In plasma-based accelerators (PBAs), an electron beam mismatched into the plasma focusing fields develops a decoherence of particle betatron oscillations and beam envelope oscillations [17-19], thus causing emittance growth. It has been shown [20-22] that beam emittance increase can be reduced by proper shaping of the longitudinal plasma density profile with smooth vacuum-plasma and plasma-vacuum transitions (up- and down-ramps). In this paper the following longitudinally-tailored profile of the plasma target is considered:

$$f(z) = \frac{1}{(1 \mp (z - z_{0,u|d})/l_{u|d})^2}, \quad (1)$$

where  $z_{0,u}$  and  $z_{0,d}$  are the longitudinal coordinates of the beginning of the up-ramp and the down-ramp respectively, and  $l_u$  and  $l_d$  are the optimized characteristic plasma ramp lengths,

$$l_{u|d} = \beta_{p0} \sqrt{\left( \frac{(N+1)\pi}{\ln(\beta_{i|goal}/\beta_{goal|i})} \right)^2 + \frac{1}{4}}. \quad (2)$$

Here  $\beta_{p0}$  is the beta function of the electron beam matched to the plasma section,  $\beta_{p0} = \sqrt{\gamma_b c m_e / (g e)}$ , where  $\gamma_b$  is the beam Lorentz factor and  $g$  is the transverse focusing field in the plasma;  $N = 0, 1, 2, \dots$ ;  $\beta_{goal}$  is the beta function of the beam matched to the plasma section in the case of the plasma up-ramp and to the external focusing elements behind the plasma accelerator stage in the case of the down-ramp; and  $\beta_i$  is the initial beam beta function. The lengths of the plasma up-ramp and down-ramp are then given by

$$L_{u|d} = (\beta_{i|goal}/\beta_{goal|i} - 1) l_{u|d}. \quad (3)$$

Such a longitudinally-tailored plasma density profile was studied for electron beam matching into and from plasma accelerators in [22] and can be experimentally implemented in appropriate gas capillaries [23].

In all simulations presented here the length of the plasma up-ramp is equal to 0.6 cm and the length of the down-ramp is equal to 0.9 cm, the length of the acceleration region is equal to 9.5 cm, and the laser pulse is focused into the plasma after the end of the plasma up-ramp.

The 3D start-to-end simulations have been carried out with the spectral quasi-cylindrical PIC code FBPIC [24]. The dimensions of the copropagating simulation window in the longitudinal and transverse directions are  $118 \times 420$   $\mu\text{m}^2$  with a resolution of  $0.022 \times 0.5$   $\mu\text{m}^2$ . The time step is 74 as, corresponding to a length of 22.19 nm. A third order particle shape function and 8 particles per cell are used for the plasma. The total number of beam particles is equal to 158280. The simulations were run in a Lorentz boosted frame with a frame relativistic factor of  $\gamma_f = 5$ . The Galilean-Pseudo-spectral analytical time-domain (Galilean-PSATD) solver [25, 26] has been used for electromagnetic field calculations. This field solver excludes the numerical Cherenkov instability (NCI) [27-29], which falsifies the simulation results.

### 3D Start-to-End Simulations

A set of start-to-end three-dimensional simulations has been conducted to examine a potential experimental setup for laser-driven plasma acceleration with external injection at SINBAD, optimize the quality of the accelerated beam and investigate the effect of the injection phase on the accelerated beam quality. The results are summarized in Table 2. The evolution of the witness electron beam properties (mean energy, relative energy spread, normalized horizontal and vertical emittances) and the laser peak normalized vector potential during injection, acceleration and extraction from the plasma is presented in Fig. 1.

In PBAs, a high-density witness beam can generate its own wakefield, beam-loading field [30, 31], which loads the longitudinal accelerating field excited by the driver. The beam-loading effect plays an important role in the energy spread evolution of an accelerated electron beam. For instance, in an extreme case of high loads, when the gradient of the beam-loading field is much higher than the gradient of the driver-induced plasma wakefield, the superposition of the two wakefields is decelerating for the witness

Content from this work may be used under the terms of the CC BY 3.0 licence (© 2019). Any distribution of this work must maintain attribution to the author(s), title of the work, publisher, and DOI

beam. Furthermore, beam loading can result in variations in the longitudinal wakefield along the witness beam position, leading to a significant growth of the beam energy spread. However, specific shaping of the electron beam charge profile or injection of the beam at a suitable phase of the wave can allow the electric field acting over the beam length to be flattened. This in turn enables the growth of the beam energy spread during the acceleration process to be mitigated.

Table 2: Parameters of the Accelerated Electron Beam After Extraction From the Plasma

$\Delta\tau_{eb/lp}$ [ $\mu\text{m}$ ]	63.4 (211.6 fs)	58.1 (193.8 fs)	52.8 (176 fs)
$I_{peak}$ [kA]	0.55	0.55	0.55
$\bar{E}$ [MeV]	1143	1065	925
$\Delta E/\bar{E}$ [%]	0.27	0.16	0.29
$\sigma_{z,rms}$ [ $\mu\text{m}$ ]	0.17	0.17	0.17
$\sigma_{x,rms}$ [ $\mu\text{m}$ ]	0.70	1.07	1.45
$\sigma_{y,rms}$ [ $\mu\text{m}$ ]	0.60	0.90	1.20
$\varepsilon_{n,x}$ [ $\mu\text{m}$ ]	0.11	0.11	0.11
$\varepsilon_{n,y}$ [ $\mu\text{m}$ ]	0.10	0.10	0.10

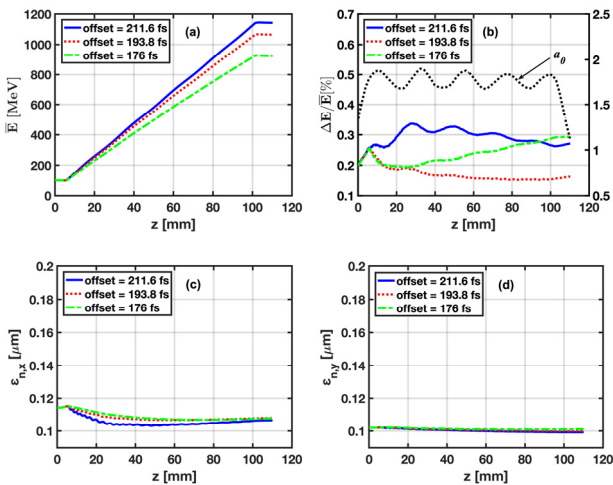


Figure 1: Evolution of the externally injected electron beam properties during acceleration to GeV energy: mean energy (a), relative energy spread (b), normalized horizontal emittance (c) and normalized vertical emittance (d). Temporal offsets between the electron beam center and the laser pulse center are equal to 211.6 fs (63.4  $\mu\text{m}$ ) – blue solid curve, 193.8 fs (58.1  $\mu\text{m}$ ) – red dotted curve and 176 fs (52.8  $\mu\text{m}$ ) – green dash-dot curve. Evolution of the peak normalized vector potential of the laser pulse during propagation through the plasma – black dotted curve (b).

In all considered cases, the beam relative energy spread slightly increases throughout the plasma up- and down-ramps [see Fig. 1(b)] due to the domination of the beam-loading field over the laser-driven plasma wakefield, since the beam density is higher than the plasma density and the laser intensity is relatively low in the regions of plasma ramps. In the cases of electron beam-laser offsets of 193.8 fs and 176 fs after the start of the beam acceleration

process, the total relative energy spread decreases due to a fast reduction in the uncorrelated relative energy spread. As described above, later the correlated energy spread growth begins to dominate over the uncorrelated energy spread decrease, resulting in a growth in the total relative energy spread of the beam injected with a temporal offset of 176 fs. Due to dephasing of the electron beam with respect to the plasma wake wave, the witness beam, injected with a temporal offset of 193.8 fs, passing through the middle of the plasma, reaches the wave phase in which the beam-loading field compensates the laser-driven wakefield, hence leading to a decrease in the beam relative energy spread. Further electron beam-laser dephasing leads to a reduction of beam loading compensation and the beam relative energy spread stays almost constant up to the end of the plasma focusing channel. After extraction from the plasma the relative energy spread of the beam is 0.16 % (a decrease from the initial value of 21 %) for a mean energy of 1.07 GeV. In the case of beam injection near the on-crest acceleration phase, from the end of the plasma up-ramp the total relative energy spread increases due to fast growth of the correlated energy spread caused by variations in the longitudinal accelerating field along the electron beam. As the witness beam slowly slips forward with respect to the plasma wave closer to the position where the beam loading effect can be compensated, these variations in the field acting on the beam tend to be flattened resulting in a reduction in the correlated energy spread growth. Later, the total relative energy spread start to decrease when the uncorrelated energy spread decrease becomes dominant over the correlated energy spread growth. In addition to the main trends in the relative energy spread evolution, it exhibits mild variations due to changes in the plasma wakefield amplitude and shape, caused by the periodic self-focusing and defocusing of the laser pulse during its propagation through the parabolic plasma channel, as shown in Fig. 1(b).

As shown in Fig. 1(c) and 1(d), the use of short plasma ramps, 0.6 cm in length at the beginning of the plasma and 0.9 cm at the plasma exit, allows both normalized horizontal and vertical emittances to be preserved during beam injection, acceleration and extraction from the plasma.

Based on the above, for the considered arrival-time jitters between the external electron beam and the laser driver of up to 35.6 fs (10.64  $\mu\text{m}$ ) after acceleration to GeV energies and extraction from the plasma, the witness beam has very promising properties with RMS-duration of around 0.55 fs, peak current of 0.55 kA, energy spread below 0.3 % and transverse normalized emittances of 0.1  $\mu\text{m}$  in both dimensions.

## CONCLUSION

A good working point has been found for a potential experimental setup for laser-driven plasma acceleration with external injection of an electron beam from an RF linac at SINBAD for ATHENA<sub>e</sub>. For the considered parameter set, the arrival-time jitter between the external electron beam and the laser driver of up to 35.6 fs does not have a significant influence on the final parameters of the accelerated electron beam.

## ACKNOWLEDGEMENTS

The authors would like to acknowledge the FBPIC developers and contributors.

## REFERENCES

- [1] E. Esarey, C. B. Schroeder, and W. P. Leemans, "Physics of laser-driven plasma-based electron accelerators", *Rev. Mod. Phys.*, vol. 81, pp. 1229–1285, 2009.
- [2] C. L. Haefner *et al.*, "High average power, diode pumped petawatt laser systems: a new generation of lasers enabling precision science and commercial applications", in *Proc. SPIE Optics + Optoelectronics*, Prague, Czech Republic, April 2017, vol. 10241, p. 1024102.  
doi:10.1117/12.228105
- [3] K. Nakamura *et al.*, "Diagnostics, Control and Performance Parameters for the BELLA High Repetition Rate Petawatt Class Laser", *IEEE J. Quantum Electron*, vol. 53, no. 4, p. 1200121, 2017.  
doi:10.1109/JQE.2017.2708601
- [4] C. E. Clayton *et al.*, "Ultra-high-Gradient Acceleration of Injected Electrons by Laser-Excited Relativistic Electron Plasma Waves", *Phys. Rev. Lett.*, vol. 70 (1), p. 37, 1993.
- [5] F. Amiranoff *et al.*, "Observation of Laser Wakefield Acceleration of Electrons", *Phys. Rev. Lett.*, vol. 81 (5), p. 995, 1998.  
<https://doi.org/10.1103/PhysRevLett.81.995>
- [6] A. R. Rossi *et al.*, "The External-Injection experiment at the SPARC\_LAB facility", *Nucl. Instr. Meth. A*, vol. 740, p. 60, 2013.  
<https://doi.org/10.1016/j.nima.2013.10.063>
- [7] B. M. G. Zeitler, "Phase Space Linearization and External Injection of Electron Bunches into Laser-Driven Plasma Wakefields at REGAE", Ph.D. thesis, Phys. Dept., Universität Hamburg, 2016.
- [8] M. J. H. Lutikhof, "Theoretical investigation of external injection schemes for laser wakefield acceleration", Ph.D. thesis, Faculty of Science and Technology, University of Twente, 2010.
- [9] M. K. Weikum, "Generation, acceleration and measurement of attosecond electron beams from laser-plasma accelerators", Ph.D. thesis, Phys. Dept., University of Strathclyde, 2017.
- [10] E. N. Svystun *et al.*, "Two-Stage Laser-Driven Plasma Acceleration with External Injection for EuPRAXIA", *J. Phys.: Conf. Ser.*, vol. 1067, p. 042011, 2018.  
doi:10.1088/1742-6596/1067/4/042011
- [11] A. R. Rossi *et al.*, "Plasma boosted electron beams for driving Free Electron Lasers", *Nucl. Instr. Meth. A*, vol. 909, p. 54, 2018.  
<https://doi.org/10.1016/j.nima.2018.02.092>
- [12] M.K. Weikum *et al.*, "Improved Electron Beam Quality from External Injection in Laser-driven Plasma Acceleration at SINBAD", in *Proc. IPAC'17*, Copenhagen, Denmark, May 2017, pp. 1707-1710.  
doi:10.18429/JACoW-IPAC2017-TUPIK013
- [13] U. Dorda *et al.*, "The Dedicated Accelerator R&D Facility Sinbad at DESY", in *Proc. IPAC'17*, Copenhagen, Denmark, May 2017, pp. 869-872.  
doi:10.18429/JACoW-IPAC2017-MOPVA012
- [14] B. Marchetti *et al.*, "Conceptual and Technical Design Aspects of Accelerators for External Injection in LWFA", *Appl. Sci.*, vol. 8 (5), p. 757, 2018.  
<https://doi.org/10.3390/app8050757>
- [15] J. Zhu *et al.*, "Sub-fs bunch generation with sub-10-fs bunch arrival time jitter via bunch slicing in a magnetic chicane", *Phys. Rev. ST Accel. Beams*, vol. 19, p. 054401, 2016.

- [16] J. Zhu, R. Assmann, U. Dorda and B. Marchetti, "Lattice design and start-to-end simulations for the ARES linac", *Nucl. Instr. Meth. A*, vol. 909, p. 467, 2018.  
<https://doi.org/10.1016/j.nima.2018.02.045>
- [17] R. Assmann and K. Yokoya, "Transverse beam dynamics in plasma-based linacs", *Nucl. Instrum. Methods Phys. Res. Sect. A*, vol. 410, pp. 544-548, 1998.  
[https://doi.org/10.1016/S0168-9002\(98\)00187-9](https://doi.org/10.1016/S0168-9002(98)00187-9)
- [18] K.A. Marsh *et al.*, "Beam Matching to a Plasma Wake Field Accelerator using a Ramped Density Profile at the Plasma Boundary", in *Proc. PAC'05* (IEEE, Piscataway, NJ, 2005), Knoxville, TN, May 2005, pp. 2702–2704.  
<https://doi.org/10.1109/PAC.2005.1591234>
- [19] A.G. Khachatryan, A. Irman, F. van Goor and K.-J. Boller, "Femtosecond electron-bunch dynamics in laser wakefields and vacuum", *Phys. Rev. ST Accel. Beams*, vol. 10, p. 121301, 2007.  
<https://doi.org/10.1103/PhysRevSTAB.10.121301>
- [20] K. Floettmann, "Adiabatic matching section for plasma accelerated beams", *Phys. Rev. ST Accel. Beams*, vol. 17, p. 054402, 2014.  
<https://doi.org/10.1103/PhysRevSTAB.17.054402>
- [21] I. Dornmair, K. Floettmann, and A. R. Maier, "Emittance conservation by tailored focusing profiles in a plasma accelerator", *Phys. Rev. ST Accel. Beams*, vol. 18, p. 041302, 2015.
- [22] X. L. Xu *et al.*, "Physics of phase space matching for staging plasma and traditional accelerator components using longitudinally tailored plasma profiles", *Phys. Rev. Lett.*, vol. 116, p. 124801, 2016.
- [23] L. Schaper *et al.*, "Longitudinal gas-density profilometry for plasma-wakefield acceleration targets", *Nucl. Instr. Meth. A*, vol. 740, pp. 208-211, 2014.  
<https://doi.org/10.1016/j.nima.2013.10.052>
- [24] R. Lehe *et al.*, "A spectral, quasi-cylindrical and dispersion-free Particle-In-Cell algorithm", *Comput. Phys. Commun.*, vol. 203, pp. 66-82, 2016.
- [25] M. Kirchen *et al.*, "Stable discrete representation of relativistically drifting plasmas", *Phys. Plasmas*, vol. 23, p. 100704, 2016.  
<https://doi.org/10.1063/1.4964770>
- [26] R. Lehe *et al.*, "Elimination of Numerical Cherenkov Instability in flowing-plasma Particle-In-Cell simulations by using Galilean coordinates", *Phys. Rev. E*, vol. 94, p. 053305, 2016.  
<https://doi.org/10.1103/PhysRevE.94.053305>
- [27] B. B. Godfrey, "Numerical Cherenkov instabilities in electromagnetic particle codes", *J. Comput. Phys.*, vol. 15, pp. 504-521, 1974.  
[https://doi.org/10.1016/0021-9991\(74\)90076-X](https://doi.org/10.1016/0021-9991(74)90076-X)
- [28] B. B. Godfrey, "Canonical momenta and numerical instabilities in particle codes", *J. Comput. Phys.*, vol. 19, pp. 58-76, 1975.  
[https://doi.org/10.1016/0021-9991\(75\)90116-3](https://doi.org/10.1016/0021-9991(75)90116-3)
- [29] X. Xu *et al.*, "Numerical instability due to relativistic plasma drift in EM-PIC simulations", *Comput. Phys. Commun.*, vol. 184, pp. 2503-2514, 2013.  
<https://doi.org/10.1016/j.cpc.2013.07.003>
- [30] S. van der Meer, "Improving the power efficiency of the plasma wakefield accelerator", CERN-PS-85-65-AA, CLICNote- 3, pp. 1-7, 1985.
- [31] T. Katsouleas *et al.*, "Beam loading in plasma accelerators", *Particle Accelerators*, vol. 22, pp. 81–99, 1987.